

THERMAL PHOTONS PRODUCTION IN PROTON-PROTON COLLISIONS AT HIGH ENERGIES

PART I. DIFFERENTIAL CROSS-SECTIONS OF PROCESSES, CALCULATED WITHOUT AND TAKING INTO ACCOUNT FORMFACTOR OF MESONS

M.R. ALIZADA, A.I. AHMADOV

Department of Theoretical Physics, Baku State University

str. Z. Khalilov, 23, Az-1148 Baku, Azerbaijan

E-mail: mohsunalizade@gmail.com

Thermal photons produced in following processes: $\pi^+\pi^- \rightarrow \gamma\rho^0$, $\pi^\pm\rho^0 \rightarrow \gamma\pi^\pm$, $\rho^0 \rightarrow \gamma\pi^+\pi^-$, $\pi^+\pi^- \rightarrow \gamma\eta$, $\pi^\pm\eta \rightarrow \gamma\pi^\pm$, $\pi^+\pi^- \rightarrow \gamma\gamma$ are considered Feynman diagrams of processes and matrix elements has been wrote. Differential cross-sections of processes has been calculated without and taking account formfactor of mesons. The dependencies of differential cross-sections of processes of production thermal photons on energy of colliding mesons (\sqrt{s}), transverse momentum (p_T) and on cosine of scattering angle of photons has been determined and has been comparised.

Keywords: proton-proton collision, mesons, thermal photons, Feynman diagram, differential cross-section.

PACS: 13.75.Lb; 13.30.Eg; 13.20.Cz; 13.25.Cq

I. INTRODUCTION

Photons are one of the main products of proton-proton collision at high energies. Photons interact only electromagnetically, and therefore their average free paths are usually much larger than the transverse size of the region of hot matter created in any nuclear collision. As a result, high energy photons formed in the interior of the plasma typically pass through the surrounding substance without interaction, carrying information directly from anywhere from where they were formed to the detector. Depending on the mechanism of their production, direct photons are usually divided into two main categories: prompt and thermal photons [1,2].

Photons produced in a proton-proton (prompt photons) collision with energy in the range from 1.5 to several *GeV* carry information about the formation of a quark gluon phase and information about distribution of partons in the nuclei. Prompt photons are formed by rigid scattering of incoming partons, such as Compton scattering of $qg \rightarrow q\gamma$ or annihilation of $q\bar{q} \rightarrow g\gamma$, as well as the braking radiation of quarks that undergo severe scattering [3,4]. These processes are described by perturbative pQCD in the LO and NLO order that dominate LHC energies. One purpose of prompt photonic measurements is to improve the accuracy of such calculations in various collision systems. In RHIC at the center of mass at energy per nucleon-nucleon pair $\sqrt{s}=0.2$ *TeV* and at LHC at $\sqrt{s}=2.76$ *TeV*, it was found that prompt photons with transverse momentum (p_T) above about 3 and 15 *GeV/c* respectively dominate fast photons and follow the power law spectral form in small systems (pp , pA , dA) as well as in heavy ion collisions as described in pQCD.

Secondary photons can be formed in reactions by mesons formed by hadrons in a proton-proton collision [6-8]. Photoproduction from light and heavy nuclei is a very effective tool for studying the interactions of mesons with nuclear substances and the properties of hadrons. The study of the electromagnetic transitions of the nucleus into unstable resonances of excitation gives a are representation of the structure of the nucleus. Excited hadrons from base quark and gluon block carry information about quark-gluon plasma. Measurement of meson production reactions from quasi-free nucleons was much more systematic, in particular by studying in detail the nuclear effect on quasi-free proton sections, which can be compared with their free counter-cell sections [5,6].

We considered thermal photons productions in the processes: $\pi^+\pi^- \rightarrow \gamma\rho^0$, $\pi^\pm\rho^0 \rightarrow \gamma\pi^\pm$, $\rho^0 \rightarrow \gamma\pi^+\pi^-$, $\pi^+\pi^- \rightarrow \gamma\eta$, $\pi^\pm\eta \rightarrow \gamma\pi^\pm$, and $\pi^+\pi^- \rightarrow \gamma\gamma$. We constructed Feynman diagrams of these processes and wrote matrix elements. Calculation of the square of matrix elements are performed using FeynCalc. The dependencies of differential cross-section of processes on energy of colliding meson, transverse momentum of p_T and cosine of scattering angle of photons has been determined. The differential sections of the processes calculated without and taking into account the meson formfactor were compared.

I. DIFFERENTIAL CROSS-SECTIONS OF THE PROCESSES

$\pi^+\pi^- \rightarrow \gamma\rho^0$, $\pi^\pm\rho^0 \rightarrow \gamma\pi^\pm$, $\rho^0 \leftarrow \gamma + \pi^+ + \pi^-$,
 $\pi^+\pi^- \rightarrow \gamma\eta$, $\pi^\pm\eta \rightarrow \gamma\pi^\pm$, $\pi^+\pi^- \rightarrow \gamma\gamma$.

WITHOUT AND TAKING INTO ACCOUNT FORMFACTOR OF MESONS

- a. differential cross-section of processes without taking into account formfactor of mesons The complete matrix element (M_I) of process $\pi^+ \pi^- \rightarrow \gamma \rho^0$ consists of the sum of the following matrix elements:
1. process $\pi^+ \pi^- \rightarrow \gamma \rho^0$

$$M_{11} = eg_s \varepsilon_\mu(k_1)(2p_1 - k_1)_\nu \frac{1}{(p_1 - k_1)^2 - m_\pi^2} (k_2 - 2p_2)_\mu \varepsilon_\nu(k_2)$$

$$M_{12} = eg_s \varepsilon_\mu(k_1)(k_1 - 2p_2)_\mu \frac{1}{(p_1 - k_2)^2 - m_\pi^2} (2p_1 - k_2)_\nu \varepsilon_\nu(k_2)$$

$$M_{13} = 2ieg_s g_{\mu\nu} \varepsilon_\mu(k_1) \varepsilon_\nu(k_2)$$

where k_1, k_2, p_1 and p_2 are momentums of photon, gluon, π^+ and π^- mesons correspondingly.

Mandelstam invariants of this process are: $s = (p_1 + p_2)^2 = (k_1 + k_2)^2$, $t = (p_1 - k_2)^2 = (p_2 - k_1)^2$, $u = (p_1 - k_1)^2 = (p_2 - k_2)^2$.

In the calculations, the product of polarization vectors was taken as follows:

photon: $\varepsilon_\mu(k_1) \varepsilon_{\mu'}^*(k_1) = -g_{\mu\mu'}$ ρ^0 meson: $\varepsilon_\nu(k_2) \varepsilon_{\nu'}^*(k_2) = -g_{\nu\nu'} + \frac{k_2^\nu \cdot k_2^{\nu'}}{m_\rho^2}$

The square of the matrix element M_I was calculated by FeynCalc at photon mass $m_\gamma=0$. The differential section of process was calculated by formula [7]:

$$\frac{d\sigma}{dt} = \frac{1}{16\pi s^2} \frac{p'_{cm}}{p_{cm}} |M_I|^2$$

where $|M_I|^2$ - square of matrix elements of the process and

$$(p_{cm})^2 = \frac{1}{4s} (s - (m_1 + m_2)^2) (s - (m_1 - m_2)^2), \quad (p'_{cm})^2 = \frac{1}{4s} (s - (m_3 + m_4)^2) (s - (m_3 - m_4)^2).$$

For process $\pi^+ + \pi^- \rightarrow \gamma + \rho^0$ masses are equal: $m_1=m_2=m_\pi$; $m_4=m_\rho$; $m_3=m_\gamma$. In estimating the differential section, Mandelstam invariants t and u were expressed through s and p_T as follows:

$$t = -\frac{s}{2}(1 - \cos(\vartheta)) + m_\rho^2 + m_\pi^2, \quad u = -\frac{s}{2}(1 + \cos(\vartheta)) + m_\rho^2 + m_\pi^2, \quad t = -p_T \sqrt{s} e^{-y},$$

$$u = -p_T \sqrt{s} e^y$$

Matrix elements of the process, taking into account the meson formfactor, are:

$$M_{11} = eg_s \varepsilon_\mu(k_1)(2p_1 - k_1)_\nu h_+(p_a) \frac{1}{(p_1 - k_1)^2 - m_\pi^2} (k_2 - 2p_2)_\mu \varepsilon_\nu(k_2)$$

$$M_{12} = eg_s \varepsilon_\mu(k_1)(k_1 - 2p_2)_\mu h_+(p_b) \frac{1}{(p_1 - k_2)^2 - m_\pi^2} (2p_1 - k_2)_\nu \varepsilon_\nu(k_2)$$

$$M_{13} = 2ieg_s a g_{\mu\nu} \varepsilon_\mu(k_1) \varepsilon_\nu(k_2)$$

where $h_+(p_a) = \frac{m_\rho^2 - m_\pi^2}{m_\rho^2 - p_a^2}$, $h_+(p_b) = \frac{m_\rho^2 - m_\pi^2}{m_\rho^2 - p_b^2}$, $a = h_+(p_a) + h_+(p_b)$, $p_a = p_1 - k_1 = k_2 - p_2$,

$$p_b = p_1 - k_2 = k_1 - p_2$$

2. process $\pi^\pm \rho^0 \rightarrow \gamma \pi^\pm$

The complete matrix element (M_2) of process $\pi^\pm \rho^0 \rightarrow \gamma \pi^\pm$ consists of the sum of the following matrix elements:

$$M_{21} = eg_s \varepsilon_\mu(k_1)(k_1 + 2p_2)_\mu \frac{1}{(p_1 + k_2)^2 - m_\pi^2} (k_2 + 2p_1)_\nu \varepsilon_\nu(k_2)$$

$$M_{22} = eg_s \varepsilon_\mu(k_1) (2p_1 - k_1)_\mu \frac{1}{(p_1 - k_1)^2 - m_\pi^2} (2p_2 - k_2)_\nu \varepsilon_\nu(k_2)$$

$$M_{23} = 2ieg_s g_{\mu\nu} \varepsilon_\mu(k_1) \varepsilon_\nu(k_2)$$

where k_1, k_2, p_1 and p_2 are momentums of photon, gluon, initial π^\pm and final π^\pm mesons correspondingly.

Mandelstam invariants of this process are: $s = (p_1 + p_2)^2 = (k_1 + k_2)^2$, $t = (p_1 - k_1)^2 = (p_2 - k_2)^2$, $u = (p_1 - k_2)^2 = (p_2 - k_1)^2$.

In the calculations, the product of the polarization vectors were taken as follows [13,14]. The square of the matrix element M_2 was calculated by FeynCalc at photon mass $m_\gamma=0$. Differential cross-section of process is calculated at: $m_1=m_4=m_\pi$, $m_2=m_\rho$; $m_3=m_\gamma$. In estimating the differential section, Mandelstam invariants t and u were expressed through s and p_T as follows:

$$t = -\frac{s}{2}(1 - \cos(\vartheta)) + m_\rho^2 + m_\pi^2, \quad u = -\frac{s}{2}(1 + \cos(\vartheta)) + m_\pi^2 + m_\pi^2, \quad t = -p_T \sqrt{s} e^{-y}, \quad u = -p_T \sqrt{s} e^y$$

Matrix elements of the process, taking into account the meson formfactor, are:

$$M_{21} = eg_s \varepsilon_\mu(k_1) (k_1 + 2p_2)_\mu h_+(p_a) \frac{1}{(p_1 + k_2)^2 - m_\pi^2} (k_2 + 2p_1)_\nu \varepsilon_\nu(k_2)$$

$$M_{22} = eg_s \varepsilon_\mu(k_1) (2p_1 - k_1)_\mu h_+(p_b) \frac{1}{(p_1 - k_1)^2 - m_\pi^2} (2p_2 - k_2)_\nu \varepsilon_\nu(k_2)$$

$$M_{23} = 2ieg_s a g_{\mu\nu} \varepsilon_\mu(k_1) \varepsilon_\nu(k_2)$$

where $h_+(p_a); h_+(p_b)$ and a have expression as (1), $p_a = p_1 + k_2 = p_2 + k_1$; $p_b = p_1 - k_1 = p_2 - k_2$.

3. process $\rho^0 \rightarrow \gamma + \pi^+ + \pi^-$

The complete matrix element (M_3) of process $\rho^0 \rightarrow \gamma + \pi^+ + \pi^-$ consists of the sum of the following matrix elements:

$$M_{31} = eg_s \varepsilon_\nu(k_2) (k_2 - 2p_2)_\nu \frac{1}{(p_1 + k_1) - m_\pi^2} (k_1 + 2p_1)_\mu \varepsilon_\mu(k_1)$$

$$M_{32} = eg_s \varepsilon_\nu(k_2) (k_2 - 2p_1)_\nu \frac{1}{(k_2 - p_1)^2 - m_\pi^2} (k_1 + 2p_2)_\mu \varepsilon_\mu(k_1)$$

$$M_{33} = 2ieg_s g_{\mu\nu} \varepsilon_\mu(k_1) \varepsilon_\nu(k_2)$$

where k_1, k_2, p_1 and p_2 are momentums of photon, gluon, π^+ and π^- mesons correspondingly.

Mandelstam invariants of this process are: $s = (p_2 + k_1)^2$, $t = (k_1 + p_1)^2$, $u = (p_1 + p_2)^2$.

In the calculations, the product of the polarization vectors were taken as follows [16,17]. The square of the matrix element M_1 was calculated by FeynCalc at photon mass $m_\gamma=0$. The differential cross-section of each process was calculated by formula [7]:

$$\frac{d\sigma}{dx_1 dx_2} = \frac{Q}{32(2\pi)^3} |M_3|^2$$

where $Q = \sqrt{k_2^2} = m_\rho$, $x_i = 2E_i/Q$ ($i = 1, 2, 3$)

In estimating the differential section, Mandelstam invariants t and u were expressed through s and p_T as follows:

$$t = -\frac{s}{2}(1 - \cos(\vartheta)) + m_\rho^2 + m_\pi^2, \quad u = -\frac{s}{2}(1 + \cos(\vartheta)) + m_\rho^2 + m_\pi^2, \quad t = -p_T \sqrt{s} e^{-y}, \quad u = -p_T \sqrt{s} e^y$$

Matrix elements of the process, taking into account the meson formfactor, are:

$$M_{31} = eg_s \varepsilon_\nu(k_2) (k_2 - 2p_2)_\nu h_+(p_a) \frac{1}{(p_1 + k_1) - m_\pi^2} (k_1 + 2p_1)_\mu \varepsilon_\mu(k_1)$$

$$M_{32} = eg_s \varepsilon_\nu(k_2) (k_2 - 2p_1)_\nu h_+(p_a) \frac{1}{(k_2 - p_1)^2 - m_\pi^2} (k_1 + 2p_2)_\mu \varepsilon_\mu(k_1)$$

$$M_{33} = 2ieg_s a g_{\mu\nu} \varepsilon_\mu(k_1) \varepsilon_\nu(k_2)$$

where $h_+(p_a); h_+(p_b)$ and a have expression as (1), $p_a = p_1 + k_1 = k_2 - p_2$; $p_b = k_2 - p_1 = p_2 + k_1$.

4. process $\pi^+ \pi^- \rightarrow \gamma \eta$

The complete matrix element (M_5) of process $\pi^+ \pi^- \rightarrow \gamma \eta$ consists of the sum of the following matrix elements:

$$M_{41} = eg_s \varepsilon_\mu(k_1) (2p_1 - k_1)_\nu \frac{1}{(p_1 - k_1)^2 - m_\pi^2} (k_2 - 2p_2)_\mu i\gamma_5(k_2)_\nu A$$

$$M_{42} = eg_s \varepsilon_\mu(k_1) (k_1 - 2p_2)_\mu \frac{1}{(p_1 - k_2)^2 - m_\pi^2} (2p_1 - k_2)_\nu i\gamma_5(k_2)_\nu A$$

$$M_{43} = 2ieg_s g_{\mu\nu} \varepsilon_\mu(k_1) i\gamma_5(k_2)_\nu A$$

where k_1, k_2 and p_1 and p_2 are momentums of photon, η, π^+ and π^- mesons correspondingly,

$$A = \lambda_u g_\pi \text{Sin}(\phi) + \lambda_s g_s \text{Cos}(\phi), \quad \lambda_u = \begin{pmatrix} 1 & 0 & 0 \\ 0 & 1 & 0 \\ 0 & 0 & 0 \end{pmatrix}, \quad \lambda_s = \begin{pmatrix} 1 & 0 & 0 \\ 0 & 1 & 0 \\ 0 & 0 & -\sqrt{2} \end{pmatrix}, \quad g_s=6,14, \quad g_\pi = \frac{m_u}{F_\pi}, \quad F_\pi=93$$

$M\partial B, \phi = 54^\circ$.

Mandelstam invariants of this process are: $s = (p_1 + p_2)^2 = (k_1 + k_2)^2$, $t = (p_1 - k_2)^2 = (p_2 - k_1)^2$, $u = (p_1 - k_1)^2 = (p_2 - k_2)^2$

In the calculations, the product of the polarization vectors were taken as follows: photon: $\varepsilon_\mu(k_1) \varepsilon_\mu^*(k_1) = -g_{\mu\mu}$

The square of the matrix element M_1 was calculated by FeynCalc at photon mass $m_\gamma=0$. For process $\pi^+ + \pi^- \rightarrow \gamma + \eta$ masses equal: $m_1=m_2=m_\pi$; $m_4=m_\eta$; $m_3=m_\gamma$. In estimating the differential section, Mandelstam invariants t and u were expressed through s and from p_T as follows:

$$t = -\frac{s}{2}(1 - \cos(\vartheta)) + m_\eta^2 + m_\pi^2, \quad u = -\frac{s}{2}(1 + \cos(\vartheta)) + m_\eta^2 + m_\pi^2, \quad t = -p_T \sqrt{s} e^{-y}, \quad u = -p_T \sqrt{s} e^y.$$

5. process $\pi^\pm \eta \rightarrow \gamma \pi^\pm$

The complete matrix element (M_6) of process $\pi^\pm \eta \rightarrow \gamma \pi^\pm$ consists of the sum of the following matrix elements:

$$M_{51} = eg_s \varepsilon_\mu(k_1) (k_1 + 2p_2)_\mu \frac{1}{(p_1 + k_2)^2 - m_\pi^2} (k_2 + 2p_1)_\nu i\gamma_5(k_2)_\nu A$$

$$M_{52} = eg_s \varepsilon_\mu(k_1) (2p_1 - k_1)_\mu \frac{1}{(p_1 - k_1)^2 - m_\pi^2} (2p_2 - k_2)_\nu i\gamma_5(k_2)_\nu A$$

$$M_{53} = 2ieg_s g_{\mu\nu} \varepsilon_\mu(k_1) i\gamma_5(k_2)_\nu A$$

where k_1, k_2 and p_1 and p_2 are momentums of photon, η , initial π^\pm and final π^\pm mesons correspondingly,

$$A = \lambda_u g_\pi \text{Sin}(\phi) + \lambda_s g_s \text{Cos}(\phi), \quad \lambda_u = \begin{pmatrix} 1 & 0 & 0 \\ 0 & 1 & 0 \\ 0 & 0 & 0 \end{pmatrix}, \quad \lambda_s = \begin{pmatrix} 1 & 0 & 0 \\ 0 & 1 & 0 \\ 0 & 0 & -\sqrt{2} \end{pmatrix}, \quad g_s=6,14, \quad g_\pi = \frac{m_u}{F_\pi}, \quad F_\pi=93$$

$MeB, \phi = 54^\circ$.

Mandelstam invariants of this process are: $s = (p_1 + p_2)^2 = (k_1 + k_2)^2$, $t = (p_1 - k_1)^2 = (p_2 - k_2)^2$ and $u = (p_1 - k_2)^2 = (p_2 - k_1)^2$.

In the calculations, the product of polarization vectors was taken as follows: for photon: $\varepsilon_\mu(k_1)\varepsilon_\mu^*(k_1) = -g_{\mu\mu}$.

The square of the matrix element M_5 was calculated by FeynCalc and at photon mass $m_\gamma=0$ it is equal. The differential cross-section of the process was calculated by the formula [9]:

$$\frac{d\sigma}{dt} = \frac{1}{16\pi s^2} \frac{p'_{cm}}{p_{cm}} |M_5|^2$$

Here $(p_{cm})^2 = \frac{1}{4s} (s - (m_1 + m_2)^2) (s - (m_1 - m_2)^2)$ и $(p'_{cm})^2 = \frac{1}{4s} (s - (m_3 + m_4)^2) (s - (m_3 - m_4)^2)$

For process $\pi^\pm + \eta \rightarrow \gamma + \pi^\pm$ masses equal: $m_1=m_4=m_\pi$; $m_2=m_\eta$; $m_3=m_\gamma$

In estimating the differential section, Mandelstam invariants t and u were expressed through s and from p_T as follows:

$$t = -\frac{s}{2}(1 - \cos(\vartheta)) + m_\eta^2 + m_\pi^2, \quad u = -\frac{s}{2}(1 + \cos(\vartheta)) + m_\pi^2 + m_\pi^2, \quad t = -p_T \sqrt{s} e^{-y}, \quad u = -p_T \sqrt{s} e^y.$$

6. process $\pi^+ \pi^- \rightarrow \gamma\gamma$

The complete matrix element (M_6) of process $\pi^+ \pi^- \rightarrow \gamma\gamma$ consists of the sum of the following matrix elements:

$$M_{61} = e^2 \varepsilon_\mu(k_1) (2p_1 - k_1)_\nu \frac{1}{(p_1 - k_1)^2 - m_\pi^2} (k_2 - 2p_2)_\mu \varepsilon_\nu(k_2)$$

$$M_{62} = e^2 \varepsilon_\mu(k_1) (k_1 - 2p_2)_\mu \frac{1}{(p_1 - k_2)^2 - m_\pi^2} (2p_1 - k_2)_\nu \varepsilon_\nu(k_2)$$

$$M_{63} = -2e^2 g_{\mu\nu} \varepsilon_\mu(k_1) \varepsilon_\nu(k_2)$$

where k_1, k_2 and p_1 and p_2 are momentums of initial photon, final photon, initial π^+ and final π^- mesons, correspondingly,

$$A = \lambda_u g_\pi \sin(\phi) + \lambda_s g_s \cos(\phi), \quad \lambda_u = \begin{pmatrix} 1 & 0 & 0 \\ 0 & 1 & 0 \\ 0 & 0 & 0 \end{pmatrix}, \quad \lambda_s = \begin{pmatrix} 1 & 0 & 0 \\ 0 & 1 & 0 \\ 0 & 0 & -\sqrt{2} \end{pmatrix}, \quad g_s = 6, 14, \quad g_\pi = \frac{m_u}{F_\pi}, \quad F_\pi = 93$$

$M \rightarrow B, \phi = 54^\circ$.

Mandelstam invariants of this process are: $s = (p_1 + p_2)^2 = (k_1 + k_2)^2$, $t = (p_1 - k_2)^2 = (p_2 - k_1)^2$, $u = (p_1 - k_1)^2 = (p_2 - k_2)^2$. In the calculations, the product of polarization vectors was taken as follows for photon: $\varepsilon_\mu(k_1)\varepsilon_\mu^*(k_1) = -g_{\mu\mu}$. The square of the matrix element M_6 was calculated by FeynCalc at photon mass $m_\gamma=0$. The differential cross-section of the process was calculated by the formula [7]:

$$\frac{d\sigma}{dt} = \frac{1}{16\pi s^2} \frac{p'_{cm}}{p_{cm}} |M_6|^2$$

here $(p_{cm})^2 = \frac{1}{4s} (s - (m_1 + m_2)^2) (s - (m_1 - m_2)^2)$ and $(p'_{cm})^2 = \frac{1}{4s} (s - (m_3 + m_4)^2) (s - (m_3 - m_4)^2)$.

For process $\pi^+ + \pi^- \rightarrow \gamma + \gamma$ mass equal: $m_1=m_2=m_\pi$; $m_3= m_4=m_\gamma$

In estimating the differential section, Mandelstam invariants t and u were expressed through s and from p_T as follows:

$$t = -\frac{s}{2}(1 - \cos(\vartheta)) + m_\pi^2, \quad u = -\frac{s}{2}(1 + \cos(\vartheta)) + m_\pi^2, \quad t = -p_T \sqrt{s} e^{-y}, \quad u = -p_T \sqrt{s} e^y.$$

III. RESULTS OF NUMERICAL CALCULATIONS AND THEIR DISCUSSION

a. the dependencies of differential cross-section of processes on energy colliding mesons, transverse momentum p_T , cosine of the scattering angle of photons and formfactor of mesons

1. process $\pi^+\pi^- \rightarrow \gamma\rho^0$

In the fig.1(a,b,c) are represents the dependence of differential cross-section of photon production $\pi^+\pi^- \rightarrow \gamma\rho^0$ process, calculated without and taking into account formfactor of mesons on energy colliding mesons \sqrt{s} , on the transverse momentum p_T and on cosine of scattering angle of photon.

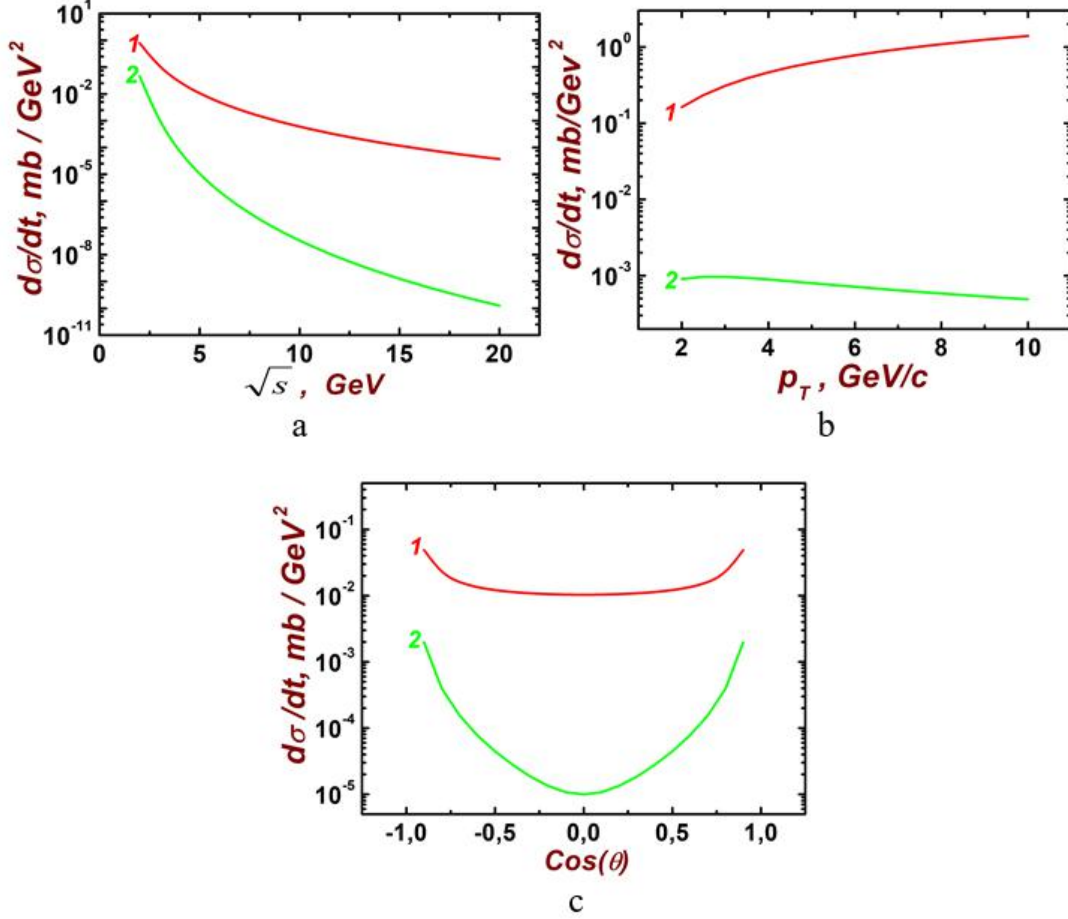


Fig. 1. (a,b,c) The dependence of differential cross-section of photon production $\pi^+\pi^- \rightarrow \gamma\rho^0$ process calculated without (curve 1) and taking into account formfactor of mesons (curve 2) on energy of colliding mesons \sqrt{s} (a), on transverse momentum p_T (b), on cosine of scattering angle of photon calculated (c) calculated without and taking into account formfactor of mesons curves 1 and 2, correspondingly.

As see from fig.1(a) the differential cross-section of processes decrease with increasing of energy of colliding π mesons. Lorentz conversion of the size of colliding particles shows that at high energies colliding particles have the shape of a disk, this in turn reduces the likelihood of colliding of constituent particles. Particles pass through each other without interaction of components. Therefore, the differential collision section is small at high energies than at low collision energies.

Differential cross-section of process increase with increasing transverse momentum p_T and at values of $p_T > 5$ GeV/c dependence to reach plateau (fig.1(b)).

As see from fig.1(c) the dependence differential cross-section of process on cosine of scattering angle of photon is symmetric relative to point $\text{Cos}(\theta)=0$ and have big value at $\text{Cos}(\theta)=\pm 1$.

The dependence differential cross-section on cosine of scattering angle of photon have minimum at $\text{Cos}(\theta)=0$ and maximums at $\text{Cos}(\theta)=\pm 1$.

Influence formfactor of meson to differential cross-section of process is significant at high values of energies of colliding mesons and transverse momentum.

The ratio of dependencies of differential cross-section on energy of colliding mesons, transverse momentum and cosine of scattering angle has been investigated. The ratio of dependencies of differential cross-sections on energy of colliding meson and ratio of dependencies of the differential cross-section on momentum p_T calculated without and taking into account the formfactor the meson is significant at large energy values of colliding mesons and transverse momentum. As ratio of $R_{II} > 1$ in all values of energy \sqrt{s} and transverse momentum p_T means

$$\frac{d\sigma_1(\pi^+\pi^-\rightarrow\gamma\rho^0)}{dt} > \frac{d\sigma_{1f}(\pi^+\pi^-\rightarrow\gamma\rho^0)}{dt} \text{ Ratio}$$

of dependencies of differential cross-sections of meson of process $\pi^+\pi^-\rightarrow\gamma\rho^0$ on cosine of scattering angle of photons calculated without and taking into account formfactor has symmetrical form relative to $\text{Cos}(\theta)=0$. It has a maximum at $\text{Cos}(\theta)=0$ and with an increase in the absolute value of the cosine of the angle of scattering of photons decreases (fig.3(c)). Taking into account the formfactor of meson in the dependence of the differential cross-section on the cosine of the scattering angle has a

large effect at small values of the cosine of the angle and a small effect at the $\text{Cos}(\theta)=\pm 1$.

2. process $\pi^\pm\rho^0\rightarrow\gamma\pi^\pm$

In the fig.2(a,b,c) represent the dependence of the differential cross-section of $\pi^\pm\rho^0\rightarrow\gamma\pi^\pm$ process on energy of colliding mesons, the transverse momentum p_T , and on the cosine of the angle of the scattering photon calculated (c) without and taking into account of formfactor of mesons.

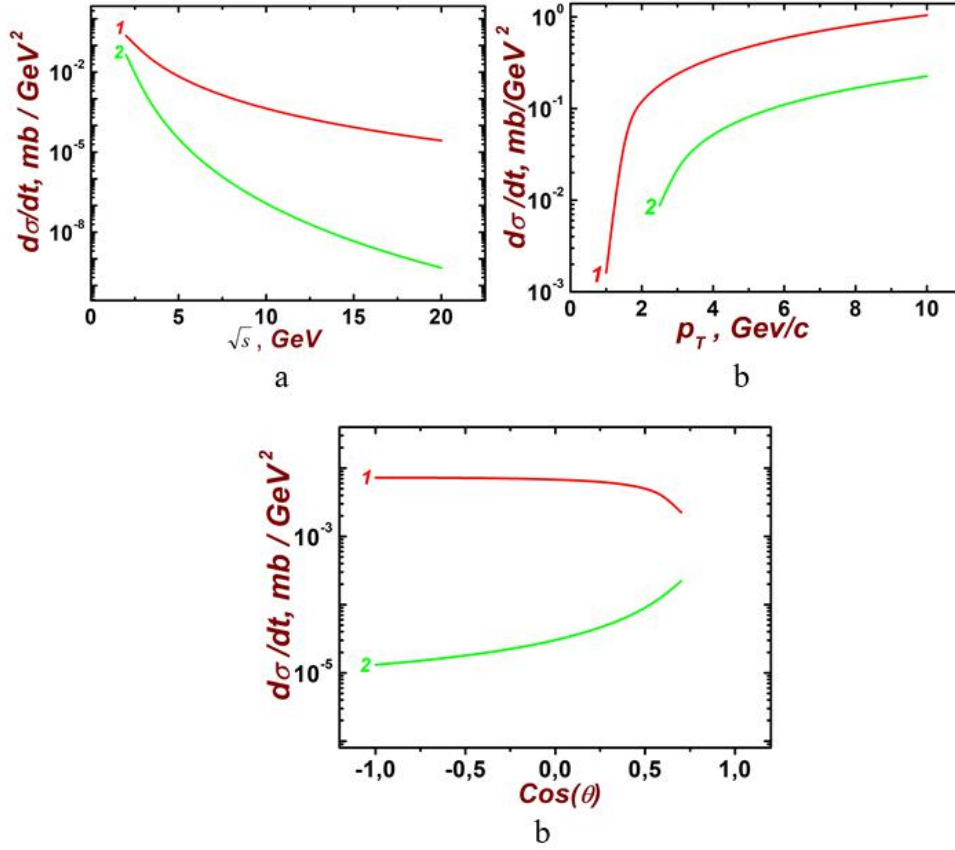


Fig.2. (a,b,c) dependence of the differential cross-section of $\pi^\pm\rho^0\rightarrow\gamma\pi^\pm$ process on energy of colliding mesons (a) and on the transverse momentum p_T (b), on the cosine of the scattering angle of the photon (c) calculated without and taking into account formfactor of mesons curves 1 and 2, correspondingly.

As can be seen from fig.2(b), the dependence of the differential cross-section on p_T is increased with increasing transverse momentum and at big values of p_T reach saturation. The dependence of the differential cross-section on the cosine of the scattering angle of photon in the interval $[-1, 0.4]$ is practically constant and in the interval $(0.4, 1]$ decreases sharply fig.3(c). Differential cross-section of process decrease with increasing transverse momentum p_T .

Differential cross-section of process decrease with increasing of energy of colliding mesons (fig.6(a)). Differential cross-section decrease with increasing transverse momentum p_T . Differential cross-section of process increase with increasing with cosine

of scattering angle of photon. Differential cross-section of process have minimum at $\text{Cos}(\theta)=-1$ and maximums at $\text{Cos}(\theta)=+1$. The dependence of differential cross-section of process on cosine of scattering angle of photon dependet on energy of colliding mesons and decrease with increasing of energy of mesons.

As ratio of $R_{1f} > 1$ in all values of energy \sqrt{s} and transverse momentum p_T means

$$\frac{d\sigma_1(\pi^\pm\rho^0\rightarrow\gamma\pi^\pm)}{dt} > \frac{d\sigma_{1f}(\pi^\pm\rho^0\rightarrow\gamma\pi^\pm)}{dt}$$

Ratio of differential cross-section on energy of colliding mesons decrease with increasing of energy.

Differential cross-section decrease with increasing cosine of scattering angle of photon.

3. process $\rho^0 \rightarrow \gamma\pi^+\pi^-$

Fig.3(a,b) represent the dependence of the differential cross-section $\rho^0 \rightarrow \gamma\pi^+\pi^-$ process on the

energy of colliding mesons, on transverse momentum p_T , and the on the cosine of scattering angle of the photon calculated at the energies of colliding mesons 5 and 10 GeV.

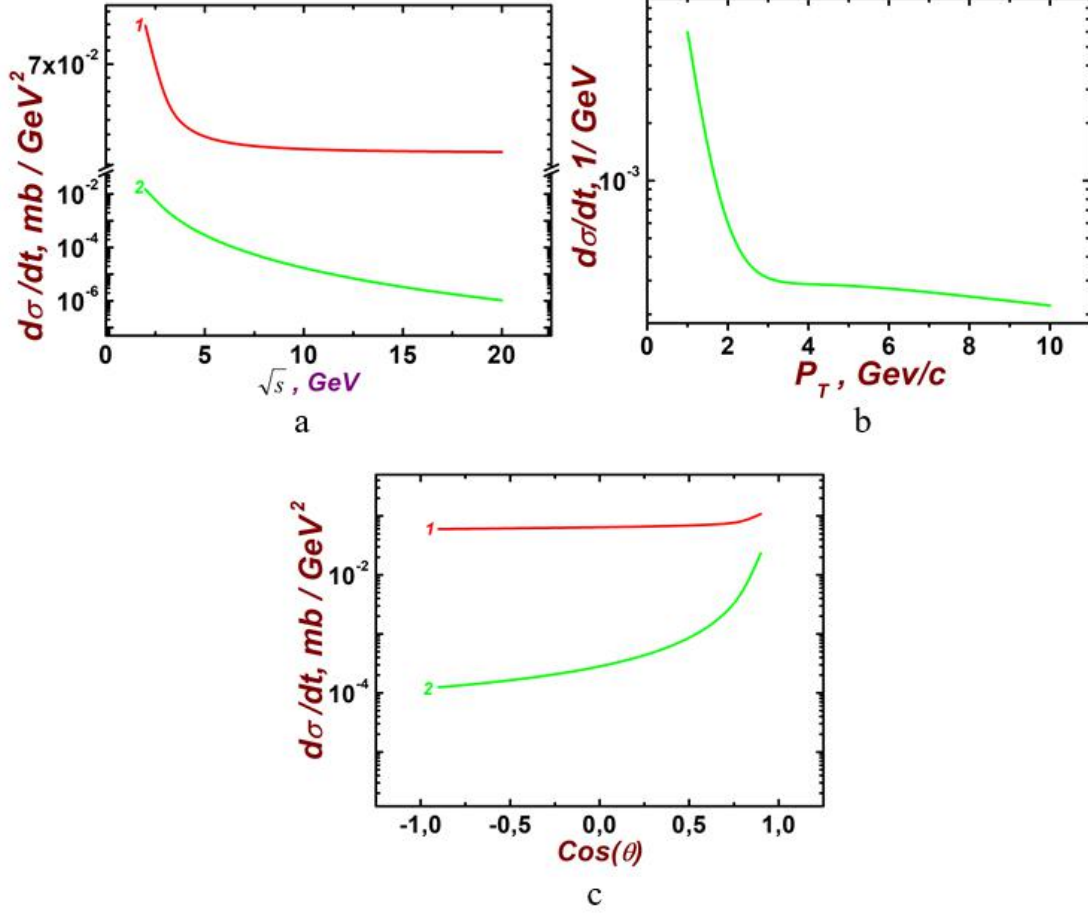


Fig.3. (a,b,c) the dependence of the differential cross section of $\rho^0 \rightarrow \gamma\pi^+\pi^-$ process on energy of colliding mesons (a), on the transverse momentum p_T (b), and on the cosine of the scattering angle of photon calculated without and taking into account formfactor of mesons curves 1 and 2, correspondingly (c).

As see from fig.3(b) the differential cross-section of process $\rho^0 \rightarrow \gamma\pi^+\pi^-$ is decreased with increasing of energy of colliding mesons. Differential cross-section of process $\rho^0 \rightarrow \gamma\pi^+\pi^-$ is decreased with increasing transverse momentum p_T . Differential cross-section of process $\rho^0 \rightarrow \gamma\pi^+\pi^-$ is decreased with increasing with increasing of the cosine of scattering angle of photon.

4. process $\pi^+\pi^- \rightarrow \gamma\eta$

Fig.4(a,b,c) represent the dependence of the differential cross-section of process $\pi^+\pi^- \rightarrow \gamma\eta$

on energy colliding mesons, on transverse momentum, and cosine of angle of scattering of photon calculated at the energies of colliding mesons 5 and 10 GeV.

As see from fig.4(b) the differential cross-section of process $\pi^+\pi^- \rightarrow \gamma\eta$ is decreased with increasing of energy of colliding mesons. Differential cross-section of process $\pi^+\pi^- \rightarrow \gamma\eta$ is decreased with increasing transverse momentum p_T . Differential cross-section of process $\pi^+\pi^- \rightarrow \gamma\eta$ does not depend on the cosine of scattering angle of photon.

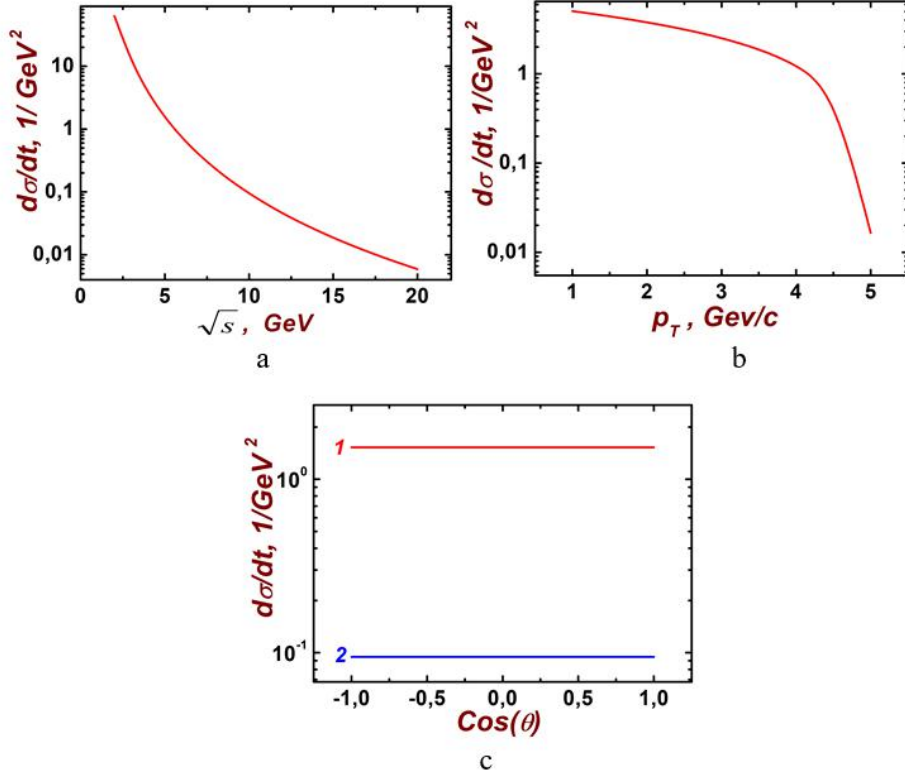


Fig.4. (a,b,c) The dependence of the differential cross-section of process $\pi^+\pi^-\rightarrow\gamma\eta$ on energy colliding mesons (a), on transverse momentum p_T (b), and cosine of angle of scattering of photon (c) calculated at energies of colliding mesons 5 and 10 GeV curves 1 and 2, correspondingly (c).

5. process $\pi^+\eta\rightarrow\gamma\pi^+$

Fig.5(a,b,c) represent the dependence of the differential cross section of process $\pi^+\eta\rightarrow\gamma\pi^+$ on the energy of colliding mesons, on transverse momentum p_T and cosine of scattering angle of photon, calculated at energies of colliding mesons 5 and 10 GeV curves 1 and 2, correspondingly.

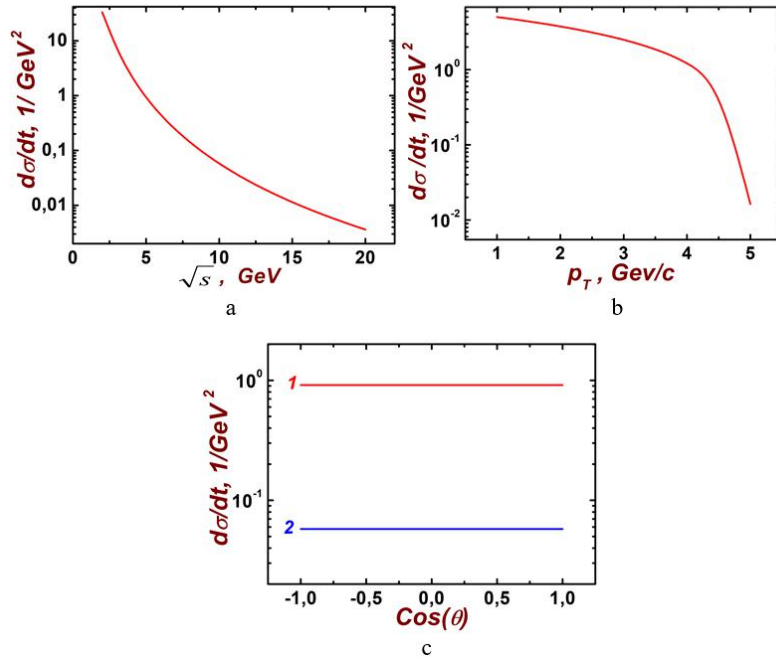


Fig. 5. (a,b,c) The dependence of the differential cross section $\pi^+\eta\rightarrow\gamma\pi^+$ process on tenergy of colliding mesons (a), on the transverse momentum p_T (b) and cosine of scattering angle of γ photon (c) calculated at energies of colliding mesons 5 and 10 GeV curves 1 and 2, correspondingly.

As see from fig.5(b) the differential cross-section of process $\pi^\pm\eta \rightarrow \gamma\pi^\pm$ is decreased with increasing of energy of colliding mesons. Differential cross-section of process $\pi^\pm\eta \rightarrow \gamma\pi^\pm$ is decreased with increasing transverse momentum p_T . Differential cross-section of process $\pi^\pm\eta \rightarrow \gamma\pi^\pm$ does not depend on the cosine of scattering angle of photon.

6. process $\pi^+\pi^- \rightarrow \gamma\gamma$

Fig.6(a,b,c) represent the dependencies of the differential cross-section of $\pi^+\pi^- \rightarrow \gamma\gamma$ process on the energy of colliding mesons, transverse momentum p_T , and on the cosine of scattering angle of photon, calculated at energies 5 and 10 GeV.

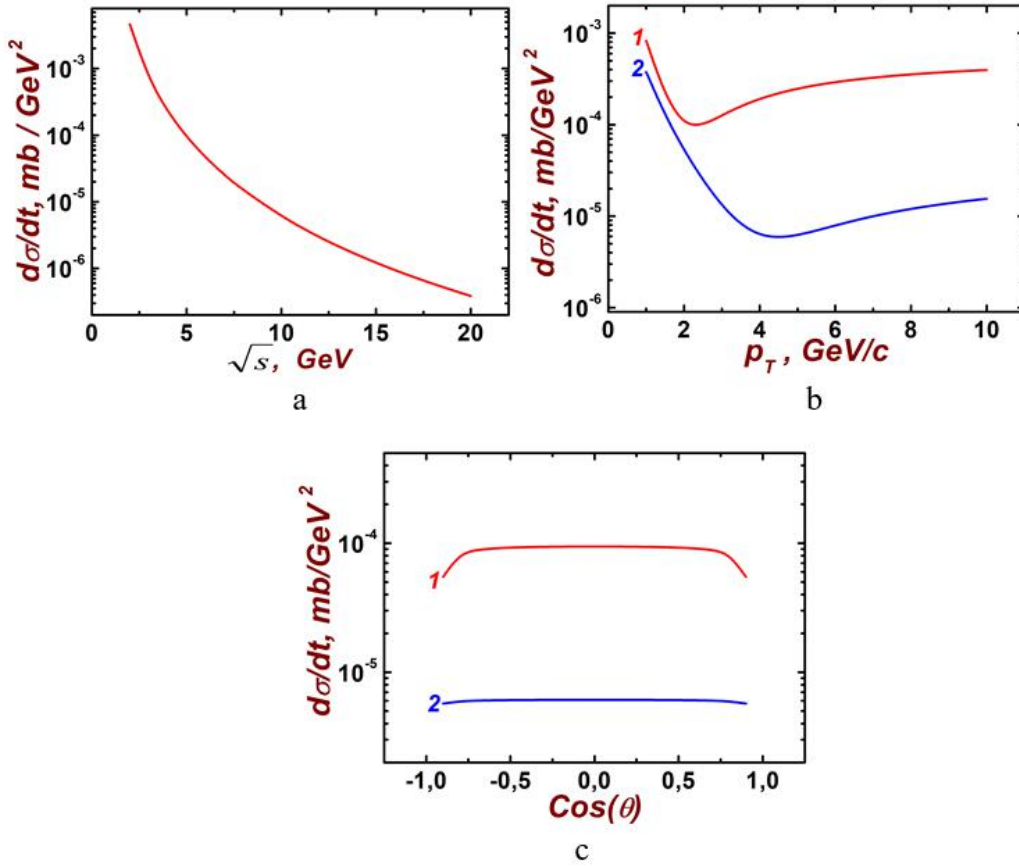


Fig.6. (a,b,c) the differential cross-section of $\pi^+\pi^- \rightarrow \gamma\gamma$ process on energy of colliding mesons (a), on the transverse momentum p_T (b), and on the cosine of the scattering angle of photon (c), calculated at energies 5 and 10 GeV.

CONCLUSIONS

It is shown that the differential cross-section of all investigated processes decreased with increasing of energy of colliding protons. The dependencies of differential cross-sections of process on transverse momentum, cosine of scattering angle of photon depend on energy of colliding mesons. The dependencies of differential cross-sections of processes decrease with increasing of energy of

The differential cross-section of process decreased with increasing of energy of colliding mesons. The dependence of differential cross-section of $\pi^+\pi^- \rightarrow \gamma\gamma$ have minimum at p_T 2.2 GeV/c and at taking into account formfactor of meson it shift to big values of p_T . The dependence of differential cross-section on cosine of scattering angle of photon in the big interval practically is constant and sharply decreases at $Cos(\theta) = \pm 1$.

The dependence differential cross-section on transverse momentum and cosine of scattering angle of photon decreases with increasing of energy of colliding mesons.

colliding mesons.

The dependence of differential cross-section on cosine of scattering angle of photons is different.

The dependence of differential cross-section of processes $\pi^+\pi^- \rightarrow \gamma\rho^0$, $\rho^0 \rightarrow \gamma\pi^+\pi^-$ and $\pi^+\pi^- \rightarrow \gamma\eta$ on cosine of the angle of scattering photons is symmetric relative to 0 and it increases with the cosine of the angle in the intervals [-1, 0) and (0, 1].

The differential cross-section of process $\pi^\pm \rho^0 \rightarrow \gamma \pi^\pm$ has a maximum at -1 cosine of the scattering angle of photons and decreases with increasing cosine of the angle scattering photons.

The differential cross-section of process $\pi^\pm \eta \rightarrow \gamma \pi^\pm$ does not depend on cosine of the angle scattering photons. It is shown that accounting of the formfactor of mesons reduces of differential cross-section of processes.

The dependence of differential cross-section on the energy of the colliding mesons calculated taking into account the formfactor of meson has lower values than without taking into account the formfactor. The

meson formfactor has a small contribution to the differential cross-section at large energies of colliding mesons. Influence formfactor of meson to differential cross-section of process depend on energy of colliding mesons. Influence of formfactor of mesons to differential cross-section of process decreased with increasing energy of colliding mesons.

All mathematical calculations were performed in Mathematica 10 and FeynCalc. Feynman diagrams are constructed using JaxoDraw 2. The graphs are constructed using the Origin 9 program and edited using the Adobe Photoshop 8 graphics editor.

-
- [1] *P. Aurenche, R. Baier, M. Fontannaz.* Phys.Rev. D 42, 1440 (1990). DOI:<https://doi.org/10.1103>.
- [2] *T. Becher, C. Lorentzen, M.D. Schwartz.* Phys. Rev. D 86, 054026 (2012). <https://doi.org/10.1103/PhysRevD.86.054026>, arXiv:1206.6115 [hep-ph].
- [3] <https://doi.org/10.48550/arXiv.1206.6115>.
- [4] *J. Kapusta, P Lichard, D Seibert.* High energy photons from quark-gluon plasma versus hot hadronic gas. Nuclear Physics A 544, 1992, 485.
- [5] *J. Kapusta, P. Lichard, D. Seibert.* High-energy photons from quark-gluon plasma versus hot hadronic gas. Phys.Rev. D 44, 2774 (1991).
- [6] *P. Arnold, G.D. Moore, L.G. Yaffe.* Photon emission from ultrarelativistic plasmas. JHEP 11, 2011, 057.
- [7] *B. Krusche1.* Photoproduction of mesons off nuclei Electromagnetic excitations of the neutron and meson-nucleus interactions. arXiv:1110.0192v1 [nucl-ex] 2 Oct (2011).
- [8] *E. Byckling, K. Kajantie.* John Wiley and Sons, London, New York, Sydney, Toronto, 1973.

Received: 14.12.2022